DOI: 10.1515/adms-2015-0018

Z. Ławrynowicz

University of Science and Technology, Mechanical Engineering Faculty, Department of Materials Science and Engineering, Av. Kaliskiego 7, 85-789 Bydgoszcz, Poland
lawry@utp.edu.pl

PLASTIC DEFORMATION AND SOFTENING OF THE SURFACE LAYER OF RAILWAY WHEEL

ABSTRACT

In this study scanning electron microscope (SEM) and optical micrograph observations were used to investigate the plastic deformation near the surface of the worn railway wheel following service. Microstructure, plastic deformation and micro-hardness of the material in the outermost tread layer of used passenger railway wheel were characterised. It was found that the material in the contact surface of wheel undergoes severe plastic deformation. Vickers micro-hardness measurements in the highly deformed layer could be correlated with softening of the outer wheel rim and the spheroidisation of the cementite phase. Examination of worn, railway wheel taken out of service, has indicated that cracks are predominantly initiated at the wheel surface down the edges of highly strained, pro-eutectoid ferrite zones (situated along prior austenite grain boundaries) and that such pro-eutectoid ferrite zones also facilitate crack propagation.

Keywords: *monoblock railway wheels, plastic deformation, cementite spheroidisation*

INTRODUCTION

In railway traffic, the material in the contact surface of both virgin rails and wheels undergo severe plastic deformation as when the train passes through curves or switches, can increase the temperature in the outermost tread layer. If the temperature reaches high enough, so that austenitisation takes place, martensitic phase transformation may take place upon cooling [1]. During the slide the temperature in the material volumes close to the contact surface will rapidly rise because of the generated friction heat. When the wheel starts rolling again, the cooling will be very efficient by heat conduction into the cold wheel material. The rapid temperature increase followed by rapid cooling causes martensite to form close to the surface. In this transformed layer, cracks are often formed which can propagate into the wheel during the service. But, also for a moderate temperature increase of a few hundred degrees, the beneficial effects of work hardening can be diminished as the material undergoes solid state reactions as recovery or recrystallisation [2].

The heat treatment of the wheels is of central importance in providing the wheel with the necessary product properties. Railway wheels are heat treated by means of a so-called rim hardening process [3]. After austenitisation at temperatures close to 900°C, only the wheel rim is rapidly cooled to temperatures of about 300°C – usually by using water. After finishing the rim quenching, centre and hub are still at temperatures near the transition temperature (Fig. 1) [4]. Further cooling takes place in the air, giving the wheel rim high strength and compressive residual stresses and producing a more flexible wheel centre. The final annealing step at about 500°C can be considered to be a stress relief treatment with no significant changes to the microstructure or the mechanical properties of the wheel material [3].

Fine-grain steels with a fine-lamellar ferrite-pearlite microstructure provides an optimal compromise between mechanical properties, wear resistance and thermal stability. Therefore, pearlitic-ferritic steels are predominantly used for railway wheels. A rail wheel typically has a wear life of about 240.000 km [4].

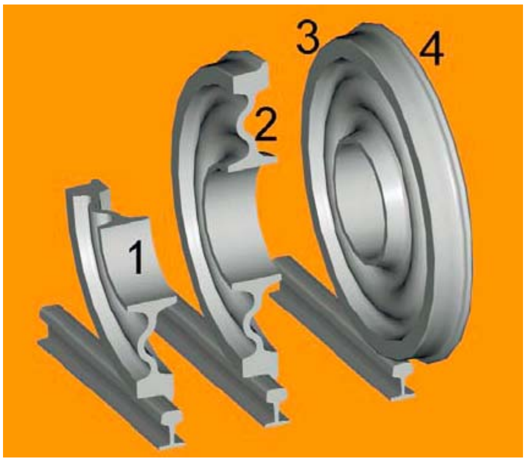

Fig. 1. Functional parts of a railway wheel: hub (1), centre (2), rim (3), with flange (4)[4]

With the advance of wheel slide protection (WSP) systems on modern passenger trains, maximum temperature in the contact is kept most often well below A_{C1} [3,4]. However, thermally induced damage to wheels caused by higher temperatures is still not uncommon [4]. Traditionally the main concern has been about martensite transformation due to its brittleness [1,4]. In mechanical analyses it is often assumed that below A_{C1} no major change of material and mechanical properties after initial work hardening will take place. The temperature below which virgin, non deformed material is not permanently deteriorated, was determined to be about 500 ^{o}C for European ER8 standard wheel steel [5]. However spheroidised pearlite has been observed during maintenance of wheels, and it is shown that temperatures in the range of approximately 500°C are present during normal running conditions [6]. Hence, thermal damage is still to be expected, but related to temperatures mainly below the alpha-gamma transformation temperature of iron.

Carbon steel with a pearlitic-ferritic microstructure is the most commonly used material for railway wheelsets due to high strength, low cost and good wear properties. However, as a result of the two-phase microstructure, pearlite is susceptible to softening at higher temperatures caused by spheroidisation of the cementite phase. The spheroidisation can eventually be more accentuated by simultaneous plastic deformation during high temperature exposure.

The aim of this work is an analysis of the structure of the material on worn surfaces of wheel with known loading histories. The change in the microstructure of wheel that occurs during loading is discussed.

MATERIAL AND EXPERIMENTAL PROCEDURES

The steel composition shown in Table 1 was, according to the European ER8 specification defined by the EN13262 standard [5]. This grade is intended for passenger train wheel sets and has a fine pearlitic-ferritic microstructure with 5 to10 vol.% free ferrite. The material was obtained from wearing wheel and specimens were extracted close to the thread in the running direction. Macro image of the view of a sample of the wheel is presented in Fig. 2. That worn wheel was after service about 250.000 km, which for a standard wheel is about 8×10^7 loading cycles [7].

Table 1. *Chemical composition of ER8 steel, wt. %*

	C	Mn	Si	P	S	Cr	Ni	Cu	Mo	V
EN 13262+A2	0.56	0.80	0.40	0.020	0.015	0.30	0.30	0.30	0.08	0.06
Experimentally determined	0.53	0.72	0.41	0.007	0.001	0.15	0.11	0.20	0.025	0.005

Evaluation of material softening was made on samples by Vickers micro-hardness indentations (HV0.1). The microstructure of metallographic sections taken from the wheel sample was characterised by light optical microscopy and by scanning JEOL JSM 5600 electron microscopy (SEM). Metallographic preparation was performed by grinding with SiC paper and diamond polishing. Etching was made with Nital (2% HNO_3 in ethanol).

Fig. 2. The view of investigated sample of monoblock wheel

Vickers micro-hardness indentation in these samples was made by Hanneman method. In order to inspect the hardness of regions of the magnitude of only tens of micrometers, a micro hardness tester using a 100 g load was utilized (HV0.1). Readings were taken at depths from 0.1 to 30 mm below the contact surface.
Fig. 3 shows a time, temperature, transition diagram for an unalloyed steel with approximately 0.5 wt.% carbon. This steel matches very well wheel steels defined by EN 13262 [5]. Three cooling paths 1-3 and the corresponding micrographs are shown. The desired cooling path for rim quenching would be somewhat to the left of path 2, crossing the

pearlite region, producing a minimum volume fraction of ferrite and leaving the bainite and martensite region untouched. The different and controlled cooling rates in the different functional parts of the wheel lead to different material properties. This allows a "material engineering" with respect to the future service conditions of the wheel. A main goal of the heat treatment process is the high homogeneity of the microstructure of the rim in a radial and circumferential direction. This is optimal for a uniform wear characteristic of the wheel tread and assures highest travelling comfort due to the prevention of wheel unroundnesses.

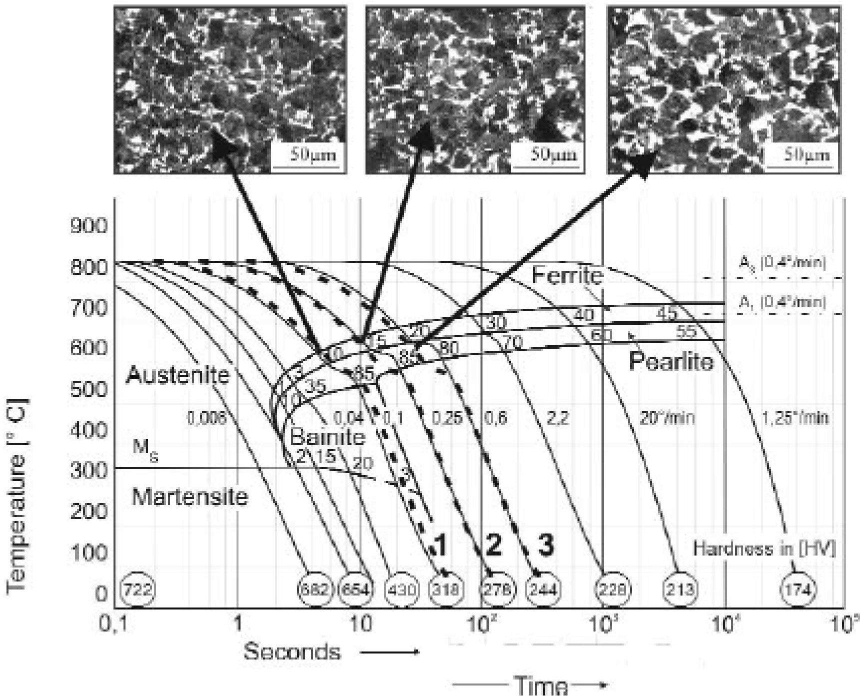

Fig. 3. Time Temperature Transformation diagram for an unalloyed steel with approximately 0.5 wt.% carbon with different cooling paths (1-3) and the corresponding micrographs [4]

RESULTS AND DISCUSSION

Typical procedures in wheel production include rim chilling with water to harden the tread surface, yielding a finer lamellar spacing in the surface; thus a small hardness gradient towards the wheel hub is always present. In the used wheel studied here, at depths below 1mm the hardness reaches close to the initial values present after production of the wheel (typically270–330 HV0.1 a few millimetres below the tread surface) indicating that the plastic deformation is small (Fig. 4).

Microhardness measurements performed on wheel rim cross-sections using micro-Vickers is shown in Fig. 4. The small increase in hardness in the surface of the wheel can be attributed to work hardening. It is well known that work hardening occurs as a result of dislocation interaction; therefore, the degree of hardening is a function of dislocation density. Micro-hardness measurements could be quantitatively correlated with the softening processes.

Softening processes present in the wheel is taken into account the simultaneous deformation and heat generation of the wheel material in the outermost layer. They include recovery or recrystallisation processes, breakdown and spheroidisation of cementite particles which could lead to an decrease of hardness of the wheel tread. Generally, these processes can influence the hardness and microstructure of the wheel material.

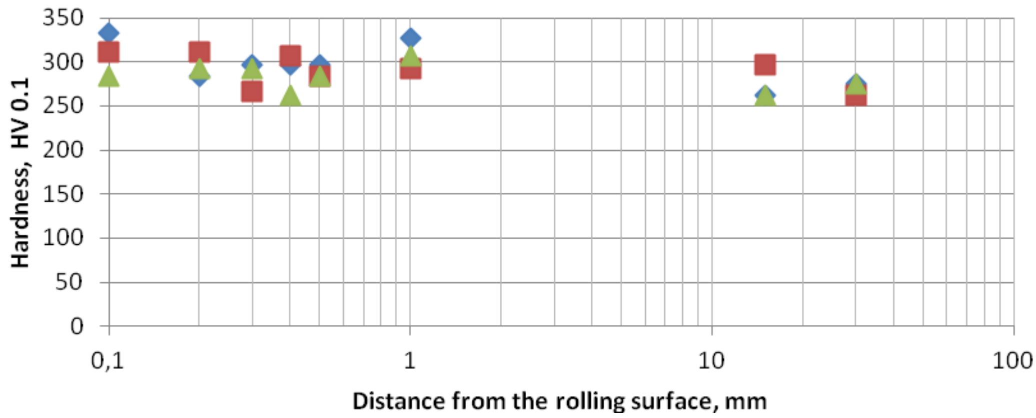

Fig. 4. Profiles of hardness from the surface down into the undeformed material

The wheel–rail contact introduces strain into the ferrite phase and at the same time produces fractures in the cementite phase beneath the contact surface. Repeated rolling contact concentrates strain in the ferrite phase that is lower in hardness than the fractured cementite [8,9]. The strain concentration forms many dislocations in the matrix ferrite, and promotes dislocation hardening and grain refinement in the matrix ferrite. As a result, the matrix ferrite is strengthened by dislocation hardening and grain refinement [10].

As the slide proceeds during wheel service, the wheel and the rail are exposed to completely different heating cycles. The contact surface on the rail is continuously exchanged and it experiences, therefore a very short heating cycle, typically a few milliseconds long. At the wheel, the contact surface is essentially the same during the entire slide, which means that heat has time to transport into the wheel and thus the temperature increases also at considerable depth under the surface. Increased temperature in the surface layers gives rise to material softening, which in combination with high shear forces cause large plastic deformations [11].

On examination of the metallographically prepared samples, it was observed that the microstructure in all the cases is pearlite and ferrite. Only the topmost layers of the wheels were affected by the wheel/rail contact. (Fig. 5). A typical representation of these structures is shown in Fig. 5a (below 15 mm from the wheel tread) and in Fig. 5b (just beneath the tread). The micrograph in Fig. 5a proves a typical ferritic–pearlitic structure, with a previous austenite grain size of approximately 20 μm (ASTM No. 8) and 9% pro-eutectoid ferrite, Fig. 6. The pro-eutectoid ferrite is not continuous, but extends around the pearlite nodules. Pro-eutectoid ferrite strain hardens more than the pearlite during exploitation.

Optical micrographs of used wheel display a heavy plastic deformation on the worn surface (Fig. 5b). As the material accumulates deformation the ductility is exhausted and the material fails as tiny flaws appear on the surface of the material. This failure mechanism is termed ratcheting failure (RF) and is different than low cycle fatigue (LCF) [12,13].

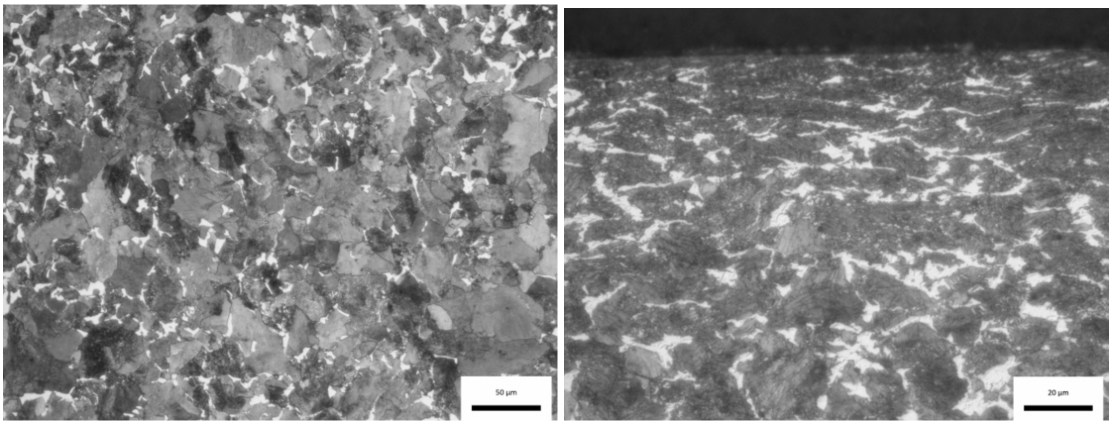

a) *b)*

Fig. 5. Undeformed (a) and deformed (b) microstructure below the contact surface of the railway wheel

The change of the volumetric content of ferrite in the rim with the distance from the rolling surface of the wheel is shown in Fig. 6. It has been reported that microstructure resembling spheroiditic appearance of pearlite near the tread surface could be produced by the combination of plastic strain from 5% to 10% and increased temperature [6,14].

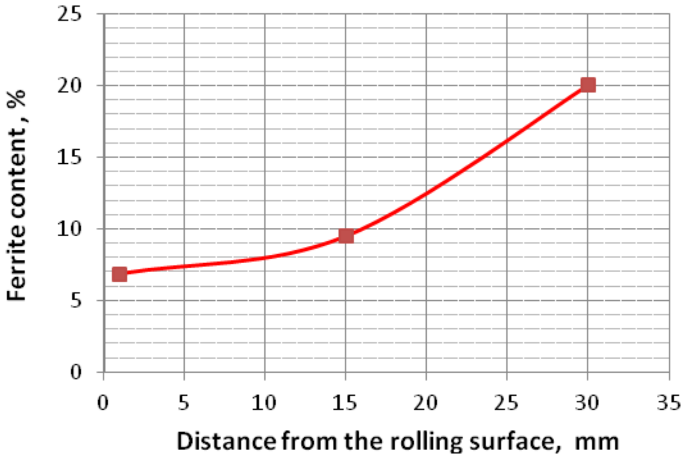

Fig. 6. The change of the volumetric content of ferrite with the distance from the rolling surface of the wheel

As Figure 7 shows, the deformation typically extends to 60 μm below the surface. The shear deformation at the surface causes the brittle cementite to break and allows the softer ferrite to be worn away. Typically cracks tend to initiate within proeutectoid ferrite and grow along the direction of the aligned most thinned ferrite regions (Fig. 7 arrowed) i.e. sheared microstructure.

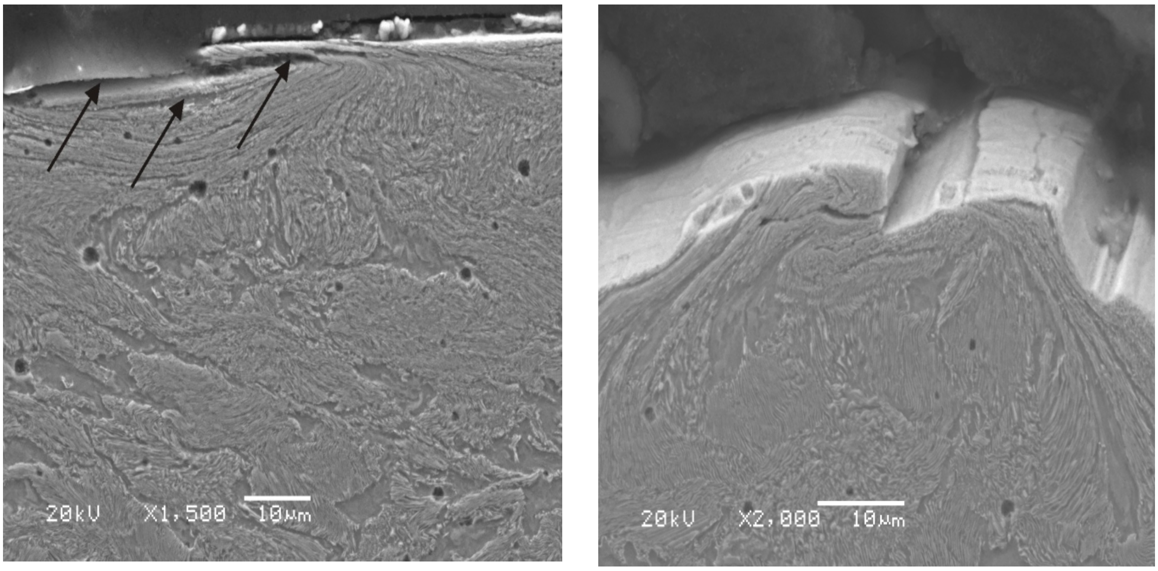

Fig. 7. Crack initiation along border of strained and flattened pro-eutectoid ferrite (arrowed) at prior austenite grain boundaries

In the outermost layer a banded structure was seen, distinguished as a fine lamellar sheared layer in SEM. Under sliding wear the microstructure evolves by the deformation and fracture of the cementite lamellae which become oriented parallel to the sliding direction at the surface. The softer ferrite is squeezed out during this process so the volume fraction of cementite close to the surface increases.

When the matrix becomes aligned the influence of the microstructure has an increased effect on crack initiation and growth [15]. Typically cracks tend to initiate within proeutectoid ferrite [16], and grow along the direction of the aligned, i.e. sheared microstructure (Fig. 7). In some areas cementite lamellas within colonies appeared to be almost disintegrated into the ferrite matrix (Fig. 8). Furthermore, it was measured that the thickness of the severely deformed surface layers is less than 200 μm. In the micro-Vickers results shown in Fig. 4, the railway wheel steel shows a small measurable hardening. This suggests that the wheel steel work hardened close to the surface only, and not far below the surface. The microstructure of the outermost layer shows material flow and plastic deformation. With increased depth (Fig. 7) shear strains decrease. Crack initiation primarily occurs along the highly strained, pro-eutectoid ferrite boundaries.

In SEM micrographs in Figs. 7 and 8 the dark etching phase of pro-eutectoid ferrite and mixed grey constituent pearlite are seeing. Spheroidised cementite lamellas are visible as discontinued globular carbide streaks within pearlite nodules. The highly deformed material in the outermost treads volume is more sensitive to softening than the non-deformed base material [10]. However, no martensite was observed of the deformed surface layer on the wheel.

These results are in agreement with similar laboratory trials, where a high amount of plastic deformation was seen to cause thermodynamic instability at elevated temperatures [17,18].

The current results take into account the simultaneous deformation and heat generation present in service, in which hardening and softening processes (dislocation generation and annihilation) can take place faster [19].

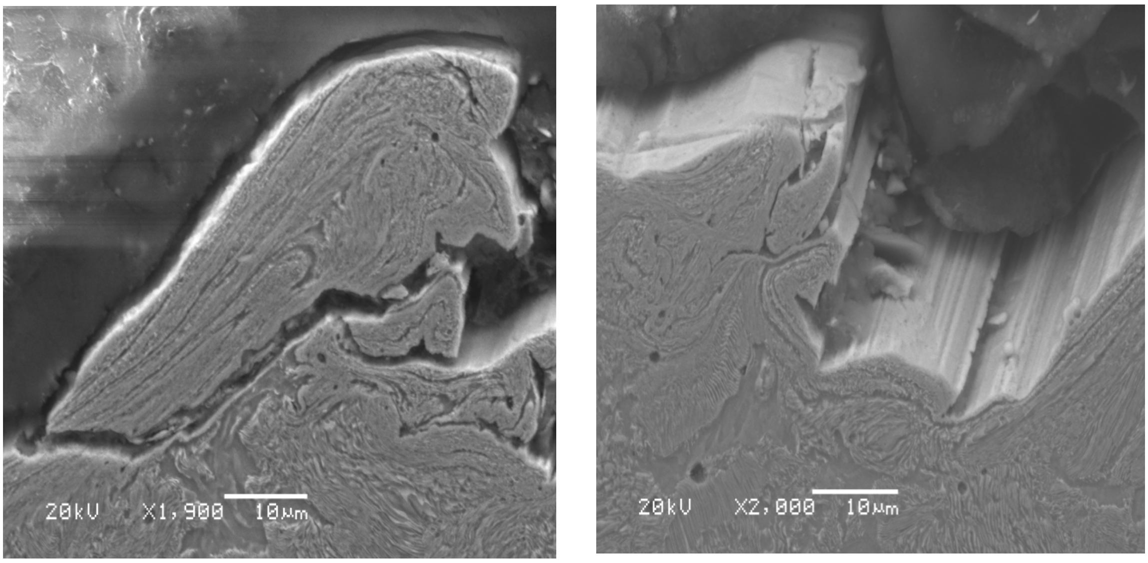

Fig. 8. Scanning electron micrographs of the wheel rim surface. The ferrite and pearlite at the wheel rim surface undergoes severe plastic deformation. Crack propagation in sub-surface zone of maximum strain with the crack 'jumping' along the edges of flattened pro-eutectoid ferrite zones

The material in the wheel tread undergoes continuous plastic deformation and thermal exposure in service. During deformation most energy will be dissipated in heat, but a small part of the energy will be stored in the material, mainly in the form of dislocation. Recovery, i.e. release of energy due to dislocation annihilation at lower temperatures will take place during service and wheel rail slide [2,6,10]. Softening caused by cementite spheroidisation in the pearlitic materials leads to changes in the mechanical behaviour.

CONCLUSIONS

In this study optical and scanning micrograph observations were used to investigate the plastic deformation and the effect of softening near the surface of the worn railway wheel following the service. It was found that the material in the contact surface of wheel undergoes severe plastic deformation. Vickers micro-hardness measurements in the highly deformed layer could be correlated with softening of the outer wheel rim and the spheroidisation of the cementite phase. Softening processes present in the wheel is taken into account the simultaneous deformation and heat generation of the wheel material in the outermost layer. They include recovery or recrystallisation processes, breakdown and spheroidisation of cement plates which could lead to a decrease of hardness of the wheel tread.

The rail–wheel contact introduces strain into the ferrite phase and at the same time produces fractures in the cementite phase beneath the contact surface. Rolling contact concentrates strain in the ferrite phase that is lower in hardness than the fractured cementite. The strain concentration forms many dislocations in the matrix ferrite, and promotes dislocation hardening and grain refinement in the matrix ferrite. As a result, the matrix ferrite is strengthened by dislocation hardening. Crack initiation primarily occurs along the highly strained, pro-eutectoid ferrite boundaries (situated along prior austenite grain boundaries) and that such pro-eutectoid ferrite zones also facilitate crack propagation.

REFERENCES

1. Alwahdi F.A.M., Kapoor A., Franklin F.J.: Subsurface microstructural analysis and mechanical properties of pearlitic rail steels in service. Wear 302 (2013), 1453–1460.
2. Cvetkovski K., Ahlström J.: Characterisation of plastic deformation and thermal softening of the surface layer of railway passenger wheel treads. Wear 300 (2013), 200–204.
3. Murawa F.: Radsätze für Schienenfahrzeuge – grundsätzliche Gedanken zur Dimensionierung. EI – Eisenbahningenieur 55 (1/2004), 40-47.
4. Poschmann I., Heermant C.: Werkstoffe für rollendes Bahnmaterial – Gefüge und mechanische Eigenschaften. EI – Eisenbahningenieur 53 (8/2002), 47-50.
5. Standard: EN 13262+A2 AUGUST 2011
6. Cvetkovski K., Ahlström J., Karlsson B.: Thermal softening of fine pearlitic steel and its effect on the fatigue behaviour. Procedia Engineering 2 (2010), 541–545.
7. Robles Hernándeza F.C. at all: Properties and microstructure of high performance wheels. Wear 271 (2011), 374–381.
8. Garnham J. E., Davis C. L.: The role of deformed rail microstructure on rolling contact fatigue initiation. Wear 265 (2008), 1363–1372.
9. Peng D., Jones R., Constable T.: A study into crack growth in a railway wheel under thermal stop brake loading spectrum. Engineering Failure Analysis 25 (2012), 280–290.
10. Ahlström J., Karlsson B.: Microstructural evaluation and interpretation of the mechanically and thermally affected zone under railway wheel flats. Wear 232 (1999), 1–14.
11. Ekberga A., Kabo E.: Fatigue of railway wheels and rails under rolling contact and thermal loading—an overview. Wear 258 (2005), 1288–1300.
12. Zerbst U., Madler K., Hintze H.: Fracture mechanics in railway applications—an overview. Engineering Fracture Mechanics 72 (2005), 163–194.
13. Fuoco R., Ferreira M.M., Azevedo C.R.F.: Failure analysis of a cast steel railway wheel. Engineering Failure Analysis 11 (2004), 817–828.
14. SHEN Xiao-hui at all: Austenite Grain Size Evolution in Railway Wheel During Multi-Stage Forging Processes. JOURNAL OF IRON AND STEEL RESEARCH, INTERNATIONAL. 20(3) (2013), 57-65.
15. Miodrag A. at all: Analysis of the spreader track wheels premature damages. Engineering Failure Analysis 20 (2012), 118–136.
16. Parida N., Das S.K., Tarafder S.: Failure analysis of railroad wheels. Engineering Failure Analysis 16 (2009), 1454–1460.
17. Ahlström J., Karlsson B.: Modelling of heat conduction and phase transformations during sliding of railway wheels. Wear 253 (2002), 291–300.
18. Donzella G. at all: Progressive damage assessment in the near-surface layer of railway wheel–rail couple under cyclic contact. Wear 271 (2011), 408–416.
19. Peng D., Jones R.: The development of combination mechanical contact and thermal braking loads for railway wheel fatigue analysis. Theoretical and Applied Fracture Mechanics 60 (2012), 10–14.